Influence of second-order Doppler effect on optical Ramsey fringe profiles

R. L. Barger

National Bureau of Standards, Boulder, Colorado 80303

Received October 14, 1980

Resolution sufficient to resolve second-order Doppler broadening (3.9 kHz) has been obtained for the Ca $^1S_0$–$^3P_1$ transition (657 nm) by using an atomic beam and optical Ramsey fringe techniques. Laser-beam separations up to 21 cm yield Ca linewidths (HWHM) as narrow as 1 kHz. As resolution is increased to approach, then exceed, the second-order linewidth, large asymmetries, shifts, and shape changes occur in the Ramsey fringe profile.

High-spectral-resolution investigations[1,2] of the Ca $^2S_0$–$^3P_1$ transition (657 nm), using an atomic beam and optical Ramsey fringe techniques, have resulted in resolution sufficient easily to resolve the second-order Doppler broadening and shift of the line (3.9-kHz width and 1.6-kHz shift for the Ca atomic beam). Interesting effects, which have not been previously observed, appear on the Ramsey fringe contour as resolution is increased to approach, then exceed, the second-order linewidth. With increasing resolution, the central fringe shifts to the red and then disappears, while the first fringe on the blue side of the pattern builds up in intensity and remains sharp for moderate resolution, the second fringe for higher resolution, etc. The side fringes become very asymmetric but retain a width much narrower than the second-order Doppler-broadened width. As discussed below, these effects arise from the different-order dependence on atomic velocity v of the second-order Doppler red shift, proportional to v^2, and the period of the Ramsey fringe for a single velocity, proportional to v.

The frequency-stabilized dye laser and Ca atomic-beam system used for this work are described in earlier papers,[1,2] which reported resolution of the 23-kHz photon-recoil doublet splitting for this Ca line. The dye-laser frequency is stabilized to have short-term rms noise of about 1 kHz and long-term drift of less than 2 kHz/h. The three-laser-beam excitation region of the atomic beam is in a transverse magnetic field of a few times 10^{-4} T (a few gauss) so that only the field-insensitive $m_j = 0$–$m_j = 0$ transition is excited. Flourescence is detected from a region located a distance $l = 10$ cm downstream.

In order to resolve second-order Doppler broadening and completely separate the fringe patterns of the two recoil peaks, beam separations larger than 7 cm (the maximum used in the earlier work) are necessary. For this, an interferometrically aligned segmented retroreflector (SRR) has been developed; it is described in detail elsewhere.[3] One SRR and an opposing cat's eye have been used for $2L = 10.5$ cm, and two opposing SRR's for $2L = 21.0$ cm.

The location of the SRR's in the experimental arrangement is indicated in Fig. 1. The SRR offsets the input beam an arbitrarily large distance and retroreflects it so that the wave fronts of the input and reflected beams are parallel to about $\lambda/10$ across the projected mode diameters. The Ramsey fringe part of the signal can be modulated by modulating the angle of the fused-quartz phase plate indicated in Fig. 1.

The fringe profiles can be calculated with sufficient accuracy for comparison with the experimental results by using Bordé's expression,[4] which is valid in the low-power limit. With approximations for this experiment (L much greater than the mode radius, small relaxation rate γ) and inclusion of the second-order Doppler shift $\Delta\nu = -(\nu_0/2)(v^2/c^2)$, the oscillating part of the Ramsey fringe profile is given by

$$I \propto \int_0^\infty dv \left\{\exp\left[-\frac{\gamma(l+L)}{v}\right]\right\}\left\{v^3 \exp\left[-\left(\frac{v}{\alpha}\right)^2\right]\right\} \times \left\{\frac{1}{v^2}\cos\left[2\pi\left(\frac{\nu-\nu_0}{\alpha/2L}+\frac{\nu_0\, v^2/2c^2}{\alpha/2L}\right)\frac{\alpha}{v}\right]\right\}, \quad (1)$$

where α is the most probable velocity (6.6×10^4 cm/sec here) and $(\nu - \nu_0)/(\alpha/2L)$ is the frequency offset normalized to the cosine period for velocity α (below, this normalized-frequency offset is referred to as δ). The velocity-dependent amplitude of the cosine consists of three factors: the upper-level decay (first bracket), the atomic-beam intensity (second bracket), and the $1/v^2$ factor (arising from the dependence of transition probability on flight time through the laser beam). For a single velocity v, the fringe cosine profile is centered

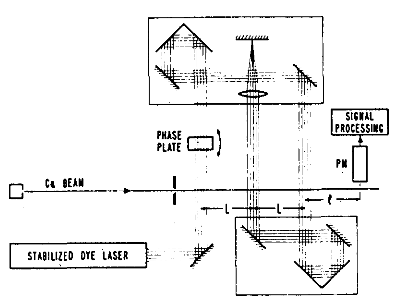

Fig. 1. Experimental arrangement using segmented retroreflectors.

0146-9592/81/030145-03$0.50/0

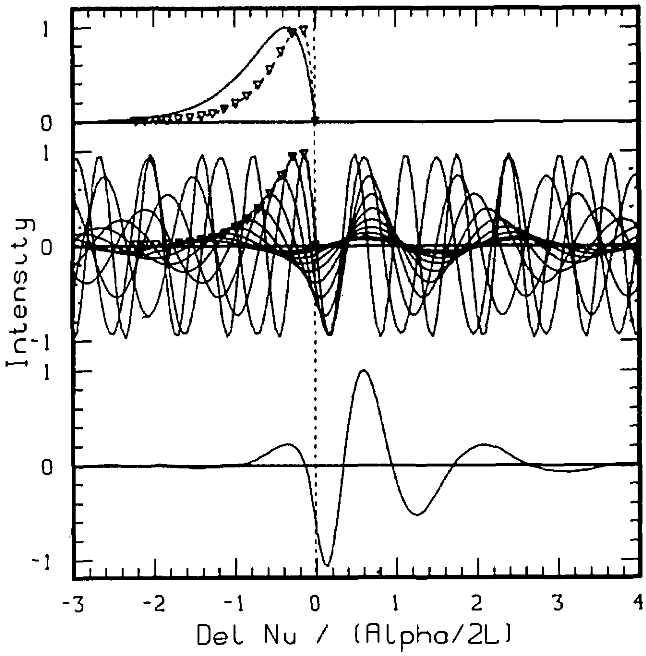

Fig. 2. Second-order Doppler distributions (upper curves), single-velocity cosine fringes (middle curves), and integrated Ramsey fringe profile (lower curve) plotted versus normalized frequency $(\nu - \nu_0)/(\alpha/2L)$ for $2L = 21.0$ cm.

at the second-order Doppler-shifted frequency $\nu_0(1 - v^2/2c^2)$ and has a period equal to $v/2L$.

The cause of the second-order Doppler-induced distortion of the Ramsey fringe is apparent in the argument of the cosine. The frequency of the intensity maximum of the Nth side fringe is $\nu - \nu_0 = Nv/2L - \nu_0 v^2/2c^2$. With high resolution (and/or high velocity), the second term, the second-order Doppler shift to the red, becomes important. As v increases, the fringes on the red side of line center (negative N) and the central fringe ($N = 0$) shift monotonically to the red, and integration over v makes these fringes broaden and integrate toward zero intensity. However, the fringes on the blue side (positive N) have the interesting characteristic of a linear shift to the blue with v and a quadratic shift to the red, and the slope of the total shift versus v curve changes sign for a turnaround velocity $v_t = Nc^2/2L\nu_0$. With this turnaround, the Nth fringes for velocities near v_t all occur at about the same frequency. If v_t is near α, integration over v can result in a strong and sharp fringe with a width much narrower than the second-order Doppler width.

The effect is illustrated with the computer-generated curves in Fig. 2. In the upper plot, the solid curve is the second-order Doppler distribution $\eta(\delta)$ for the atomic beam, i.e., the relative atomic-beam intensity of atoms with a second-order Doppler shift between δ and $\delta + d\delta$. The dashed curve is this distribution weighted by the remaining cosine amplitude factors in Eq. (1). Both distributions are normalized to 1. The middle plot shows the single-velocity cosine fringes for the velocity slices indicated by the triangular symbols, with the cosine amplitudes weighted in accordance with the dashed distribution curve. The near superposition of the $N = +1$ side fringes is apparent, with the turnaround occurring for $v = 1.4\alpha$ [$\Delta\nu/(\alpha/2L) = 0.71$]. Integration over v gives the Ramsey fringe pattern shown in the lower plot. The strongest fringe is well defined but asymmetric and is shifted a large amount to the blue.

For this resolution, the $N = 1$ fringe obtains the greatest contrast since the turnaround velocity 1.4α is near the maximum of the velocity distribution. For the fringe $N = 2$, the turnaround velocity 2.8α is at a low point of the distribution. The resulting intensities of the cosine fringes for this group of velocities are too low to build up a strong fringe but do result in the weak secondary fringe near the normalized frequency 2.1.

This behavior as a function of resolution is illustrated in the contour plot of Fig. 3. The arrows on the Z axis indicate values of Z for which experimental data have been obtained. The plot clearly illustrates that, with increasing resolving power, the central fringe disappears as the $N = 1$ blue-side fringe builds up, then the $N = 1$ fringe disappears as the $N = 2$ builds up, etc. Each fringe retains a width characteristic of the fringe for no Doppler broadening even when this is many times narrower than second-order Doppler $\eta(\delta)$ distribution. Also, the fringe intensity does not decrease dramatically with resolution, being reduced only by a factor of about 2 for $Z = 7$.

The fringe profiles including both photon-recoil components are compared with experimental results in Fig. 4, in which intensity versus frequency offset is plotted for the four laser-beam separations $2L = 3.5, 7.0, 10.5$, and 21.0 cm. The unshifted line centers for the two recoil peaks, separated by 23 kHz, are indicated by the two vertical dashed lines. The data were obtained

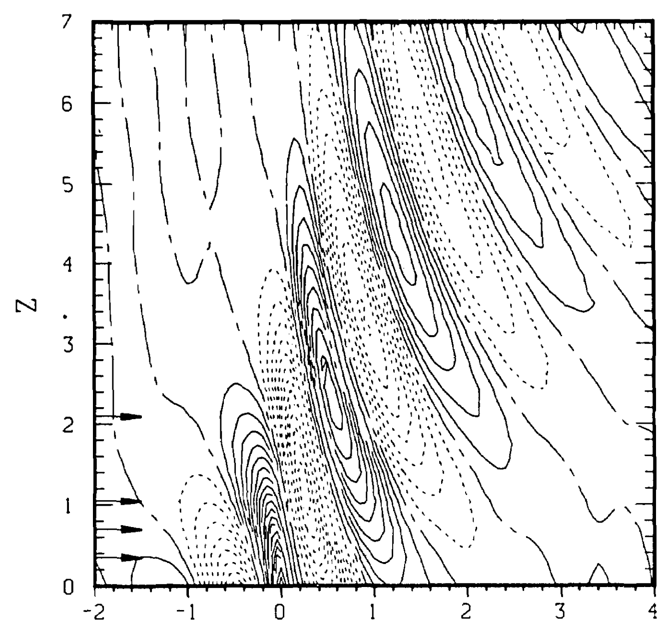

Fig. 3. Contour plot of Ramsey fringe intensity versus normalized frequency $(\nu - \nu_0)/(\alpha/2L)$ as a function of resolution. The resolution parameter Z is the ratio [FWHM of second-order Doppler distribution $\eta(\delta)$/FWHM of Ramsey fringe that would be obtained in the absence of the second-order Doppler shift]. Contour interval, 5%. Intensities: —, positive; - - -, negative; -·-, zero.

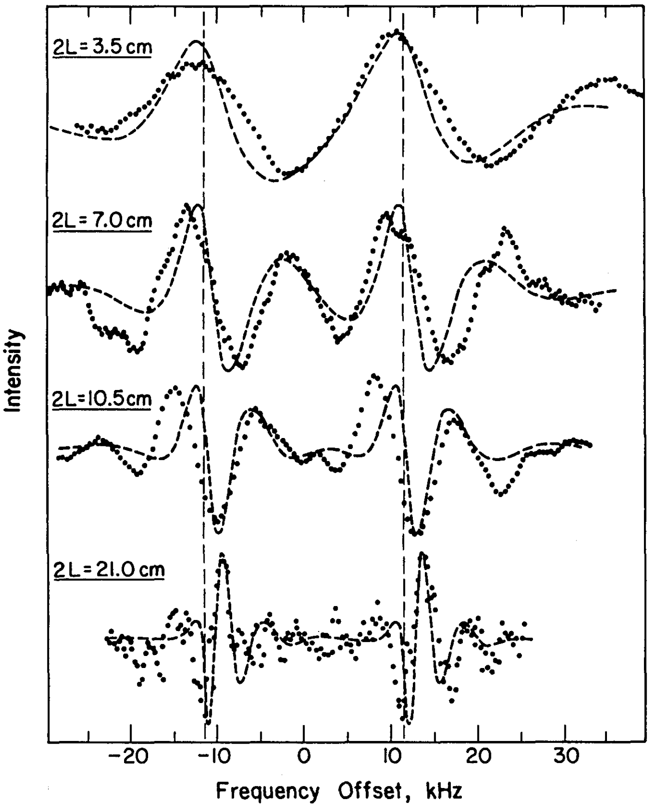

Fig. 4. Comparison between experimental (·····) and theoretical (- - -) optical Ramsey fringe profiles.

with signal-averaging techniques as described in Ref. 1, and integration times up to a few minutes were used. The broad background that was due to the atomic-beam collimation width and the single-zone saturation dip has been subtracted to leave the fringe profiles on a level baseline. The data have been slightly smoothed to improve the signal-to-noise ratio (S/N), and the peak intensity of each profile has been normalized to 1. Since in these experiments the experimental frequency scale was not accurately determined, the scales for the data have been adjusted to give the best fit between the experimental and calculated profiles. The data for $2L = 3.5$ and 7.0 cm were obtained without frequency modulation; for $2L = 10.5$ cm with frequency modulation, first derivative detection, and subsequent integration; and for $2L = 21.0$ cm with modulation of the relative phases of the laser beams and phase-sensitive detection.

It is apparent from Fig. 4 that there is reasonable agreement between theory and the experimental results. The fringe asymmetry and shift caused by the second-order Doppler effect is already present for the lowest resolution used, $2L = 3.5$ cm and $Z = 0.35$. As predicted, the fringes become shifted and very asymmetric with increasing resolution but remain sharp. Fringes with HWHM intensity as small as 1 kHz have been obtained for the highest resolution used, $2L = 21$ cm and $Z = 2.1$ (with an approximate half-intensity defined as half the difference between the peak height and the average of the heights of the two adjacent minima). This is about the width to be expected in the absence of second-order Doppler broadening.

The S/N is seen to be greatly degraded for $2L = 21.0$ cm. With the optical Ramsey fringe technique, S/N should not be greatly reduced as resolution is increased,[5] and resolution of the second-order Doppler broadening should reduce the fringe height ($I_{\max} - I_{\min}$) by only about 10% for this value of $2L$, as seen in Fig. 3. Thus the degraded S/N is believed to be due either to slight nonparallelism of the laser beams or to the residual laser-frequency jitter (the rms jitter is approximately equal to the linewidth for this resolution). With improved techniques, it should be possible to reduce the rms jitter to a few tens of hertz (Ref. 6) and to improve[1] the S/N to about 10^6.

These experimental profiles have been obtained with moderate laser powers, about 1 mW (power density about 9 mW/cm^2). With higher power, higher-velocity atoms are excited, the velocity-dependent cosine amplitudes in Eq. (1) are changed, and integration produces a changed profile. Thus the second-order Doppler effect causes power-dependent as well as resolution-dependent asymmetry and shift in Ramsey fringes. For accurate measurement of the line frequency, these effects make it imperative either that velocity selection be used so that the Ramsey fringe for a single velocity can be observed or that laser cooling of the atomic beam be used so that the second-order Doppler effect is reduced to an unimportant level.

The author would like to express his appreciation to his long-term colleague J. L. Hall for helpful discussions and constructive criticisms of this work and also to J. C. Bergquist and D. J. Glaze for contributions in the early phase of the experiments.

References

1. R. L. Barger *et al.*, Appl. Phys. Lett. **34**, 850 (1979).
2. J. C. Bergquist, R. L. Barger, and D. J. Glaze, in *Laser Spectroscopy IV* (Springer-Verlag, New York, 1979), p. 120.
3. R. L. Barger, Appl. Opt. **19**, 2088 (1980).
4. C. J. Bordé, in *Laser Spectroscopy III* (Springer-Verlag, New York, 1977), p. 121.
5. Y. V. Baklanov, B. Y. Dubetski, and V. P. Chebotayev, Appl. Phys. **9**, 171 (1976); J. C. Bergquist, S. A. Lee, and J. L. Hall, in *Laser Spectroscopy III* (Springer-Verlag, New York, 1977), p. 142.
6. R. W. P. Drever, J. L. Hall, F. W. Kowalski, J. Hough, G. M. Ford, and R. J. Munly, Joint Institute for Laboratory Astrophysics, Boulder, Colo. 80309 (in preparation).